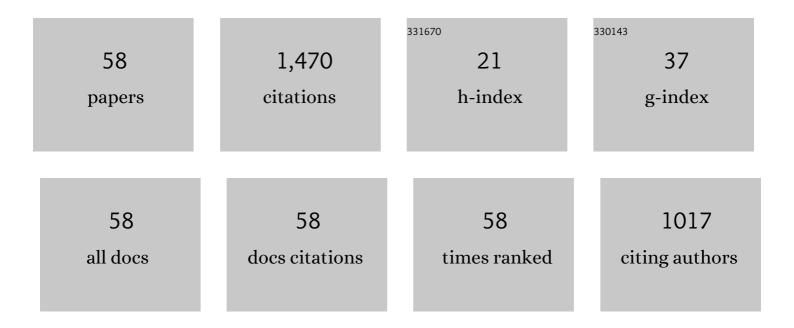
Zheng Han

List of Publications by Year in descending order

Source: https://exaly.com/author-pdf/3528961/publications.pdf Version: 2024-02-01



ΖΗΕΝΟ ΗΛΝ

#	Article	IF	CITATIONS
1	Characteristics, mechanisms, and post-disaster lessons of the delayed semi-diagenetic landslide in Hanyuan, Sichuan, China. Landslides, 2022, 19, 437-449.	5.4	7
2	Simulating the impact of highway construction to landslides with creep deformation using DDA: a case study of Qinglong landslide in Guizhou Province, China. Arabian Journal of Geosciences, 2022, 15, 1.	1.3	0
3	Extreme climate and tectonic controls on the generation of a large-scale, low-frequency debris flow. Catena, 2022, 212, 106086.	5.0	5
4	A novel multiphase segmentation method for interpreting the 3D mesoscopic structure of asphalt mixture using CT images. Construction and Building Materials, 2022, 327, 127010.	7.2	8
5	Spatiotemporal assessment of landslide susceptibility in Southern Sichuan, China using SA-DBN, PSO-DBN and SSA-DBN models compared with DBN model. Advances in Space Research, 2022, 69, 3071-3087.	2.6	17
6	Back analysis of shear strength parameters for progressive landslides: case study of the Caifengyan landslide, China. Bulletin of Engineering Geology and the Environment, 2022, 81, 1.	3.5	3
7	Hierarchical Statistics-Based Nonlinear Vertical Velocity Distribution of Debris Flow and Its Application in Entrainment Estimation. Water (Switzerland), 2022, 14, 1352.	2.7	0
8	Computer Vision-Based Hazard Identification of Construction Site Using Visual Relationship Detection and Ontology. Buildings, 2022, 12, 857.	3.1	8
9	Analysis of secondary-factor combinations of landslides using improved association rule algorithms: a case study of Kitakyushu in Japan. Geomatics, Natural Hazards and Risk, 2021, 12, 1885-1904.	4.3	4
10	Surrogate-Based Stochastic Multiobjective Optimization for Coastal Aquifer Management under Parameter Uncertainty. Water Resources Management, 2021, 35, 1479-1497.	3.9	5
11	Hydrodynamic and topography based cellular automaton model for simulating debris flow run-out extent and entrainment behavior. Water Research, 2021, 193, 116872.	11.3	9
12	A variable weight combination model for prediction on landslide displacement using AR model, LSTM model, and SVM model: a case study of the Xinming landslide in China. Environmental Earth Sciences, 2021, 80, 1.	2.7	15
13	Failure mechanism of the Yaoba loess landslide on March 5, 2020: the early-spring dry spell in Southwest China. Landslides, 2021, 18, 3183-3195.	5.4	8
14	New insights into the delayed initiation of a debris flow in southwest China. Natural Hazards, 2021, 108, 2855-2877.	3.4	2
15	Vision-Based Crack Detection of Asphalt Pavement Using Deep Convolutional Neural Network. Iranian Journal of Science and Technology - Transactions of Civil Engineering, 2021, 45, 2047-2055.	1.9	14
16	Aggravation of debris flow disaster by extreme climate and engineering: a case study of the Tongzilin Gully, Southwestern Sichuan Province, China. Natural Hazards, 2021, 109, 237-253.	3.4	10
17	Exploring the Detection Accuracy of Concrete Cracks Using Various CNN Models. Advances in Materials Science and Engineering, 2021, 2021, 1-11.	1.8	13
18	GIS-Based Three-Dimensional SPH Simulation for the 11 April 2018 Yabakei Landslide at Oita Nakatsu, Japan. Water (Switzerland), 2021, 13, 3012.	2.7	6

Zheng Han

#	Article	IF	CITATIONS
19	Landslide Susceptibility Mapping Based on the Deep Belief Network: A Case Study in Sichuan Province, China. ICL Contribution To Landslide Disaster Risk Reduction, 2021, , 201-213.	0.3	1
20	Spatiotemporal Landslide Susceptibility Mapping Incorporating the Effects of Heavy Rainfall: A Case Study of the Heavy Rainfall in August 2021 in Kitakyushu, Fukuoka, Japan. Water (Switzerland), 2021, 13, 3312.	2.7	4
21	Generation of Homogeneous Slope Units Using a Novel Object-Oriented Multi-Resolution Segmentation Method. Water (Switzerland), 2021, 13, 3422.	2.7	5
22	Improved landslide assessment using support vector machine with bagging, boosting, and stacking ensemble machine learning framework in a mountainous watershed, Japan. Landslides, 2020, 17, 641-658.	5.4	294
23	Comprehensive assessment of geological hazard safety along railway engineering using a novel method: a case study of the Sichuan-Tibet railway, China. Geomatics, Natural Hazards and Risk, 2020, 11, 1-21.	4.3	29
24	Deep Learning-Based Safety Helmet Detection in Engineering Management Based on Convolutional Neural Networks. Advances in Civil Engineering, 2020, 2020, 1-10.	0.7	49
25	Modeling the progressive entrainment of bed sediment by viscous debris flows using the three-dimensional SC-HBP-SPH method. Water Research, 2020, 182, 116031.	11.3	27
26	Mapping the susceptibility to landslides based on the deep belief network: a case study in Sichuan Province, China. Natural Hazards, 2020, 103, 3239-3261.	3.4	40
27	Spatial Proximity-Based Geographically Weighted Regression Model for Landslide Susceptibility Assessment: A Case Study of Qingchuan Area, China. Applied Sciences (Switzerland), 2020, 10, 1107.	2.5	41
28	Exploring the Impact of Multitemporal DEM Data on the Susceptibility Mapping of Landslides. Applied Sciences (Switzerland), 2020, 10, 2518.	2.5	17
29	An enhanced image binarization method incorporating with Monte-Carlo simulation. Journal of Central South University, 2019, 26, 1661-1671.	3.0	12
30	Comprehensive analysis of landslide stability and related countermeasures: a case study of the Lanmuxi landslide in China. Scientific Reports, 2019, 9, 12407.	3.3	11
31	Numerical simulation of debris-flow behavior based on the SPH method incorporating the Herschel-Bulkley-Papanastasiou rheology model. Engineering Geology, 2019, 255, 26-36.	6.3	65
32	Prediction on landslide displacement using a new combination model: a case study of Qinglong landslide in China. Natural Hazards, 2019, 96, 1121-1139.	3.4	29
33	Practical application of the coupled DDA-SPH method in dynamic modeling for the formation of landslide dam. Landslides, 2019, 16, 1021-1032.	5.4	33
34	Noncontact detection of earthquake-induced landslides by an enhanced image binarization method incorporating with Monte-Carlo simulation. Geomatics, Natural Hazards and Risk, 2019, 10, 219-241.	4.3	21
35	Protecting highway bridges against debris flows using lateral berms: a case study of the 2008 and 2011 Cheyang debris flow events, China. Geomatics, Natural Hazards and Risk, 2018, 9, 196-210.	4.3	4
36	A new DDA model for kinematic analyses of rockslides on complex 3-D terrain. Bulletin of Engineering Geology and the Environment, 2018, 77, 555-571.	3.5	24

Zheng Han

#	Article	IF	CITATIONS
37	An integrated method for rapid estimation of the valley incision by debris flows. Engineering Geology, 2018, 232, 34-45.	6.3	25
38	Development mechanism for the landslide at Xinlu Village, Chongqing, China. Landslides, 2018, 15, 2075-2081.	5.4	20
39	Research on Fault Cutting Algorithm of the Three-Dimensional Numerical Manifold Method. International Journal of Geomechanics, 2017, 17, .	2.7	11
40	Numerical simulation for run-out extent of debris flows using an improved cellular automaton model. Bulletin of Engineering Geology and the Environment, 2017, 76, 961-974.	3.5	18
41	Numerical Simulation of Post-Entrainment Debris Flow at Alluvial Fan Using FLO-2D Model. , 2017, , 311-321.		2
42	Semiautomatic Landslide Detection Using Remote Sensing and Slope Units. Transportation Research Record, 2017, 2604, 104-110.	1.9	2
43	Spatial Distribution Features of Debris Flows at Active Fault Zone Along Ya-Lu Highway, China. Open Civil Engineering Journal, 2017, 11, 563-571.	0.8	0
44	Estimating the mud depth of debris flow in a natural river channel: a theoretical approach and its engineering application. Environmental Earth Sciences, 2016, 75, 1.	2.7	5
45	3D numerical simulation of debris-flow motion using SPH method incorporating non-Newtonian fluid behavior. Natural Hazards, 2016, 81, 1981-1998.	3.4	71
46	A new algorithm to identify contact types between arbitrarily shaped polyhedral blocks for three-dimensional discontinuous deformation analysis. Computers and Geotechnics, 2016, 80, 1-15.	4.7	29
47	Extension of three-dimensional discontinuous deformation analysis to frictional-cohesive materials. International Journal of Rock Mechanics and Minings Sciences, 2016, 86, 65-79.	5.8	22
48	Elementary analysis on the bed-sediment entrainment by debris flow and its application using the TopFlowDF model. Geomatics, Natural Hazards and Risk, 2016, 7, 764-785.	4.3	16
49	Extensions of edge-to-edge contact model in three-dimensional discontinuous deformation analysis for friction analysis. Computers and Geotechnics, 2016, 71, 261-275.	4.7	41
50	A method for estimating the bed-sediment entrainment in debris flow. Japanese Geotechnical Society Special Publication, 2016, 2, 1089-1093.	0.2	0
51	Assessing entrainment of bed material in a debrisâ€flow event: a theoretical approach incorporating Monte Carlo method. Earth Surface Processes and Landforms, 2015, 40, 1877-1890.	2.5	28
52	Numerical simulation of debris-flow behavior incorporating a dynamic method for estimating the entrainment. Engineering Geology, 2015, 190, 52-64.	6.3	70
53	Detection of contacts between three-dimensional polyhedral blocks for discontinuous deformation analysis. International Journal of Rock Mechanics and Minings Sciences, 2015, 78, 57-73.	5.8	57
54	Exploring the velocity distribution of debris flows: An iteration algorithm based approach for complex cross-sections. Geomorphology, 2015, 241, 72-82.	2.6	26

ZHENG HAN

#	Article	IF	CITATIONS
55	Estimation of lateral force acting on piles to stabilize landslides. Natural Hazards, 2015, 79, 1981-2003.	3.4	24
56	DDA validation of the mobility of earthquake-induced landslides. Engineering Geology, 2015, 194, 38-51.	6.3	126
57	A hybrid automatic thresholding approach using panchromatic imagery for rapid mapping of landslides. GIScience and Remote Sensing, 2014, 51, 710-730.	5.9	12
58	A new approach for analyzing the velocity distribution of debris flows at typical cross-sections. Natural Hazards, 2014, 74, 2053-2070.	3.4	25